Geochemistry of Late Cretaceous–Paleogene potassic rocks of the early evolutionary stage in the Kamchatka island arc

Article *in* Petrology · March 2001

CITATIONS
11

READS
81

3 authors:

Gleb. Borisovich. Flerov
Institute Of Volcanology And Seismology
46 PUBLICATIONS **193** CITATIONS
SEE PROFILE

Petr Fedorov
Geological institute of Russian Academy of Sciences, Moscow
27 PUBLICATIONS **142** CITATIONS
SEE PROFILE

Tatiana Churikova
Institute Of Volcanology And Seismology
232 PUBLICATIONS **1,650** CITATIONS
SEE PROFILE

Petrology, Vol. 9, No. 2, 2001, pp. 161–178. Translated from Petrologiya, Vol. 9, No. 2, 2001, pp. 189–208.

Geochemistry of Late Cretaceous–Paleogene Potassic Rocks of the Early Evolutionary Stage in the Kamchatka Island Arc

G. B. Flerov*, P. I. Fedorov, and T. G. Churikova***

* *Institute of Volcanic Geology and Geochemistry, Far East Division, Russian Academy of Sciences, bul'v. Piipa 9, Petropavlovsk-Kamchatskii, 683006 Russia*
e-mail: fler@kcs.iks.ru

** *Geological Institute, Russian Academy of Sciences, Pyzhevskii per. 7, Moscow, 109017 Russia*
e-mail: fedorov@geo.tv-sing.ru

Received August 28, 2000

Abstract—The first data are reported on the isotopic and trace-element composition of potassic igneous rocks from central Kamchatka. The composition of minerals and distribution of incompatible elements in volcanic (shoshonitic and potassic alkaline series) and intrusive (including differentiated gabbro–syenite and trachybasalt–latite pairs) rocks testify to the comagmatic character of members of the volcano–plutonic associations and the derivation of their parental melts from a single primary magma source. The low HFSE concentrations of the rocks, as compared with those of MORB, and their low Sr and high Nd isotopic ratios suggest that the mantle source was similar to MORB. The high LILE concentrations of the rocks point to the involvement of a fluid component, which was introduced into the melts during their primary magma evolution.

INTRODUCTION

The evolution of shoshonitic magmatism in island-arc and continental-margin environments is commonly related to the rear parts of the subduction zones (Nicholls and Whitford, 1983; Edward *et al.*, 1994; Green and Lus, 2000), rifting within island arcs (Bloomer *et al.*, 1989; Rogers, 1985; Aslan, 2000), or collision-related processes (Houseman and England, 1992; Turner *et al.*, 1996). The wide occurrence of shoshonitic volcanics in ensialic island arcs with high crustal thicknesses suggests that these rocks resulted from the contamination of crustal rocks with mantle melts (Gill, 1981, *Magmaticheskie...*, 1987; Meen, 1987).

The following epochs were marked by potassic volcanic activity within the Kuril–Kamchatka island arc: the Pliocene–Quaternary in the axial and western parts of the Sredinnyi Range and western Kamchatka (Tsvetkov *et al.*, 1993; Volynets *et al.*, 1987) and the Late Eocene–Pliocene in the northern segment of the Kamchatka arc, including the Pakhachinskii Range and the Belaya River area (Kepezhinskas, 1995; Koloskov *et al.*, 1999). Analogous rocks of Late Cretaceous–Paleogene age were described in the Olyutorskaya zone of the Koryak Upland (Fedorov and Kazimirov, 1989), Sredinnyi Range in Kamchatka (Flerov and Koloskov, 1976), and the Little Kuril Islands (Tsvetkov *et al.*, 1993). Alkaline ultramafic rocks of Late Cretaceous age are exposed in the Valaginskii and Tumrok ranges within the Eastern Volcanic Belt (Seliverstov *et al.*, 1994; Markovskii and Rotman, 1971). Hence, occurrences of potassic alkaline magmas are spread throughout the whole Kamchatka segment of the Kuril–Kamchatka island arc, and this fact makes it impossible to unequivocally relate them to continental-crust thickening toward the rear parts of the arc. According to geophysical data, the thickness of the continental crust beneath the central Sredinnyi Range in Kamchatka is about 40 km, and the Benioff seismic zone boundary is traced to depths of 200 km and more (*Aktivnye vulkany Kamchatki*, 1991). The Late Cretaceous–Paleogene potassic volcanic and intrusive complexes of the Kuril–Kamchatka alkaline province were produced in a period transitional from the preorogenic to island-arc stage of the Alpine tectonic cycle. The potassic volcanics were demonstrated to belong to within-plate volcanism in an island-arc system during the onset of rifting (Tomson and Seliverstov, 1992; Koloskov *et al.*, 1999; Flerov and Seliverstov, 1999).

The aim of this study was to analyze geochemical data on the Late Cretaceous–Paleogene rocks of the potassic volcano-plutonic association of the early evolutionary stage in the Kamchatka island arc. Characteristic geological, petrological, and mineralogical features of the volcanic and plutonic rocks were described in much detail elsewhere (Flerov and Koloskov, 1976; Flerov and Seliverstov, 1999), so that we present here only the most general information on these problems.

ANALYTICAL DATA AND TECHNIQUES

This paper reports new data on the chemistry of the rocks. All of these data were obtained by precise modern techniques. Some information on the major- and trace-element composition of these rocks was published earlier (Flerov and Koloskov, 1976; Leonova and

Table 1. Representative analyses of potassic volcanic rocks from central Kamchatka

Component	g95-10c	g95-1c	3307-1	g95-3	3419g	g95-7a	3316g	t95-5g	t95-4g	3340-5
	1	2	3	4	5	6	7	8	9	10
SiO_2	44.68	44.95	45.89	46.00	47.60	49.96	50.70	52.24	52.39	57.54
TiO_2	1.55	1.65	1.60	1.60	0.60	0.69	0.70	0.90	0.83	0.43
Al_2O_3	15.87	15.22	15.85	15.50	14.20	15.33	15.60	15.85	15.95	15.84
Fe_2O_3	4.54	4.05	5.03	–	–	6.55	–	5.55	4.87	–
FeO	6.59	6.77	5.40	11.15	10.30	3.62	8.80	3.89	4.23	6.32
MnO	0.16	0.16	0.25	0.20	0.20	0.14	0.10	0.18	0.17	0.14
MgO	7.00	7.24	7.72	6.40	8.00	5.12	5.80	5.20	5.08	3.40
CaO	10.62	10.98	11.10	12.50	10.20	8.76	8.50	7.40	7.40	3.71
Na_2O	2.64	4.11	1.85	1.60	2.80	2.10	1.80	3.69	3.00	3.84
K_2O	3.54	2.23	2.35	2.20	2.10	4.80	5.00	3.90	4.50	5.60
P_2O_5	0.46	0.45	0.36	0.40	0.20	0.50	0.50	0.55	0.52	0.34
H_2O^-	–	–	0.60	–	–	0.54	–	–	–	–
LOI	2.00	1.87	2.43	–	–	2.12	–	0.62	0.54	–
Total	99.95	99.68	100.43	97.90	96.20	100.20	97.50	99.97	99.48	97.16
Cr	61	95	130	77	254	106	104	28	41	24
Ni	31	32	25	41	48	51	38	16	18	14
Co	25	38	39	14	36	30	32	24	27	21
Sc	40	34	45	45	39	37	35	22	22	21
V	376	354	–	373	288	352	271	251	244	217
Cs	1.90	1.80	0.68	1.45	0.99	1.10	1.17	1.80	2.80	0.63
Rb	39	56	–	30	41	81	91	64	79	70
Sr	523	474	403	591	981	478	438	871	1143	457
Ba	841	1172	687	716	620	1445	1353	1050	1324	641
Be	0.60	0.50	–	0.62	0.40	0.50	0.80	1.30	1.30	1.00
Y	18	17	–	20	13	14	14	23	21	12
Zr	47	43	–	54	41	36	46	81	60	53
Hf	1.90	1.65	1.42	1.81	1.12	1.01	1.59	2.95	2.30	1.46
Ta	0.50	0.20	0.42	0.34	0.08	0.17	0.34	0.40	0.50	0.17
Nb	7.10	4.80	–	7.00	0.70	3.10	4.60	4.60	4.20	2.00
U	0.60	0.30	0.26	0.28	0.31	0.42	0.55	0.80	0.70	0.24
Th	0.80	0.80	0.81	0.73	0.47	1.00	1.08	2.30	2.00	0.64
La	5.30	5.40	5.77	5.72	6.80	4.97	4.00	13.70	13.00	3.10
Ce	14.80	14.20	14.18	13.98	15.30	9.90	11.41	33.30	29.30	7.70
Pr	2.40	2.20	–	2.25	2.50	1.33	1.10	4.50	4.30	1.10
Nd	12.55	11.10	9.56	11.87	12.10	6.62	6.10	21.00	19.05	5.50
Sm	3.75	3.40	2.79	3.76	3.12	2.53	2.20	5.15	4.85	1.78
Eu	1.30	1.20	0.98	1.27	1.00	1.00	0.78	1.70	1.60	0.60
Gd	3.75	3.30	–	3.61	2.70	2.22	2.20	4.75	4.20	1.90
Tb	0.67	0.60	0.60	0.61	0.46	0.37	0.48	0.82	0.72	0.38
Dy	3.85	3.30	–	3.56	2.70	2.20	2.30	4.55	3.95	2.10
Ho	0.75	0.66	–	0.70	0.60	0.46	0.50	0.87	0.81	0.50
Er	2.00	1.80	–	1.97	1.50	1.38	1.60	2.60	2.40	1.40
Tm	0.30	0.28	–	0.27	0.20	0.21	0.30	0.41	0.35	0.20
Yb	1.80	1.70	1.71	1.68	1.60	1.35	1.50	2.70	2.20	1.50
Lu	0.26	0.24	0.24	0.23	0.30	0.20	0.20	0.37	0.34	0.30

Table 1. (Contd.)

Component	g3274-3	3253	3177-1	3164	K95-14g	3445	3310-9a	3310-13	3060-1	3341g
	11	12	13	14	15	16	17	18	19	20
SiO_2	54.60	48.88	47.16	48.94	47.46	48.70	50.20	51.20	44.44	47.30
TiO_2	0.80	0.80	0.80	0.72	1.09	0.56	0.70	0.60	0.76	0.40
Al_2O_3	15.15	9.18	12.44	12.15	11.14	12.99	14.20	15.20	5.05	5.60
Fe_2O_3	5.36	5.13	5.41	4.55	6.26	5.96	–	–	5.24	–
FeO	3.65	4.76	4.58	5.66	5.90	5.26	11.50	10.60	6.06	10.60
MnO	0.18	0.25	0.21	0.23	0.22	0.25	0.20	0.20	0.15	0.20
MgO	3.94	9.70	5.41	6.20	8.70	5.42	4.10	3.50	13.27	13.40
CaO	7.76	12.69	13.52	10.94	10.74	10.16	7.80	7.50	15.65	16.30
Na_2O	1.89	2.60	2.82	2.38	1.71	1.58	1.80	2.30	0.50	0.50
K_2O	3.47	1.30	3.28	4.80	4.01	6.84	5.00	6.30	0.90	1.50
P_2O_5	0.41	0.38	0.64	0.60	0.52	0.79	0.50	0.60	0.30	0.30
H_2O^-	0.80	–	0.40	0.66	–	0.22	–	–	0.85	–
LOI	2.27	3.30	2.24	2.13	1.91	1.69	–	–	2.97	–
Total	100.28	98.97	98.91	99.96	99.66	100.42	96.00	98.10	99.98	96.10
Cr	36	468	138	179	190	45	38	32	637	617
Ni	16	94	30	31	41	16	18	23	160	135
Co	33	44	37	36	45	39	38	30	56	51
Sc	22	42	32	31	39	29	25	24	55	61
V	–	–	–	–	365	–	273	209	235	215
Cs	0.78	1.00	0.90	1.20	0.70	1.82	0.72	–	1.11	1.28
Rb	–	–	–	–	65	109	122	102	16	27
Sr	957	224	297	639	846	730	1120	1056	229	249
Ba	1374	412	717	1214	792	1102	1342	1319	217	335
Be	–	–	–	–	0.80	1.30	1.40	1.65	0.46	0.36
Y	–	–	–	–	20	16	15	19	8	9
Zr	–	–	–	–	42	–	64	69	24	23
Hf	1.29	0.95	1.11	1.15	1.65	1.52	1.49	1.70	0.58	0.63
Ta	0.16	0.08	0.14	0.11	0.20	0.15	0.44	0.18	0.03	0.03
Nb	–	–	–	–	2.80	2.20	2.40	3.60	0.50	0.50
U	0.58	0.26	0.78	0.28	0.30	0.66	0.63	0.69	0.16	0.16
Th	1.16	0.74	0.74	0.82	0.70	1.21	0.84	1.40	0.29	0.32
La	6.69	4.92	5.63	4.88	4.60	7.20	8.47	9.35	2.15	2.01
Ce	15.45	12.07	13.23	12.09	12.40	16.30	15.30	20.58	5.51	5.26
Pr	–	–	–	–	2.00	2.50	2.30	2.86	0.94	0.90
Nd	9.33	7.50	8.43	6.43	10.30	12.00	11.10	13.78	4.78	4.71
Sm	2.96	2.29	2.66	2.13	3.30	3.43	3.30	4.18	1.49	1.67
Eu	0.88	0.70	0.85	0.72	1.10	1.20	1.10	1.45	0.48	0.54
Gd	–	–	–	–	3.60	3.50	3.10	3.47	1.53	1.65
Tb	0.48	0.39	0.48	0.43	0.69	0.63	0.50	0.54	0.26	0.28
Dy	–	–	–	–	3.95	3.40	3.00	2.95	1.51	1.63
Ho	–	–	–	–	0.80	0.60	0.50	0.60	0.31	0.32
Er	–	–	–	–	2.40	1.70	1.60	1.72	0.89	0.91
Tm	–	–	–	–	0.37	0.20	0.20	0.25	0.13	0.13
Yb	1.50	1.18	1.39	1.41	2.15	1.70	1.60	1.68	0.74	0.81
Lu	0.21	0.17	0.20	0.21	0.32	1.30	0.20	0.26	0.11	0.12

Note: (1–12) Shoshonitic series: (1–4) basalts with elevated TiO_2 concentrations, (5) basalt, (6, 7) trachybasalt, (8, 9) trachybasaltic andesite, (10) latite, (11) monzonite from a dike, (12) porphyritic pyroxenite from a dike; (13–20) potassic alkaline series: (13 and 14) absarokite, (15, 16) shonkinite, (17, 18) epileucite shonkinite, (19) leucite-bearing analcime shonkinite porphyry, (20) orthoclase pyroxenite from a sill. (1–4 and 8) Saranskaya River, (9, 10, 15, 16, and 20) Kirganik River, (5, 13, and 14) Zhupanka River, (11 and 12) Andrianovka River, (7, 17, and 18) Bogdanovskaya River, (19) Chengnuta River. Analyses 13 and 20 additionally contain 0.89 and 3.84% CO_2, respectively. Dashes mean not determined. Here and in Table 2, oxides are given in wt %, trace elements are in ppm.

Flerov, 1977; Fedorov and Dubik, 1990; Koloskov *et al.*, 1999; Flerov and Seliverstov, 1999).

All major and some trace elements (Table 1) were analyzed in 38 samples by XRF techniques at the Geochemical Institute of the George August University in Goettingen, Germany, and in 13 samples by conventional chemical techniques at the Institute of Volcanology, Far East Division, Russian Academy of Sciences. If the concentrations of trace elements were <30 ppm, they were analyzed in the 35 samples by ICP-MS at Geochemical Institute of the George August University in Goettingen, Germany, and, in seven samples, by INAA at the Geochemical Laboratory of the Cornell University, Itaky, United States. All analyses were conducted in compliance with conventional techniques (Churikova *et al.*, 2000) and display reproducibility within the errors of the respective analytical techniques.

The Sr and Nd isotopic composition was determined in 16 monomineralic separates of clinopyroxene from the volcanic and intrusive rocks and in two whole-rock syenite samples at the Laboratory of isotopic geochemistry of the Institute of the Geology of Ore Deposits, Petrography, Mineralogy, and Geochemistry, Russian Academy of Sciences, (analysts V.N. Golubev and D.Z. Zhuravlev) with a correction for an age of 50 Ma. All analyses were carried out by the technique described by Koloskov *et al.* (2001).

PETROGRAPHY AND MINERALOGY

The potassic basaltoid volcano-plutonic association is most fully represented in the central portion of the Sredinnyi Range in Kamchatka. Exposures of the rocks are traced, as a discontinuous stripe, along the eastern slope of the Sredinnyi Range from the upper reaches of the Kirganik River in the north to the Ozernaya Kamchatka River in the south (Fig. 1). The magmatic association includes lavas, subvolcanic bodies, and dikes, as well as volcano-sedimentary and sedimentary rocks, which compose the Kirganik Formation. The formation has a Paleogene age and is subdivided into three units: lower volcanogenic, middle sedimentary, and upper volcanogenic. The volcanics comprise two rock series: plagioclase subalkaline shoshonitic and plagioclase-free potassic alkali-basaltic. The rocks of both series occur within the same areas and are found throughout the stratigraphic succession of the formation, but there is a general tendency of an increase in the potassium concentrations of the alkaline rocks toward the stratigraphic top of the section, which contains more subvolcanic rocks of the potassic alkaline association. The alkaline basaltic volcanism of the Late Cretaceous–Paleogene stage in central Kamchatka was concluded with massive potassic metasomatism, which was structurally restricted to the necks of Kirganik fossil volcanoes (Flerov and Koloskov, 1976).

The intrusive complex comprises dunite, pyroxenite, gabbro (early magmatic phases), syenites, and monzonites (late phases), which compose both polyfacies and simple massifs of corresponding composition (Flerov and Koloskov, 1976). The intrusions are exposed within the area of the Kirganik Formation, among volcano-siliceous rocks of the underlying Irunei Formation of Late Cretaceous age, and metamorphic rocks of the Sredinnyi Massif (Fig. 1).

The shoshonitic series includes basalts, high-Ti basalts, trachybasalts, trachybasaltic andesites, latites, essexites, and dikes of porphyritic pyroxenites. The basaltoids and latites persistently carry phenocrysts of plagioclase, salite (up to diopside in some varieties), magnetite, and, sometimes, biotite or, very rarely, hornblende. The composition of clinopyroxene phenocrysts varies within the range $Wo_{44.5-50}En_{35-50}Fs_{4-17}$, K_{mg} = 67–93, Cr_2O_3 = 0–0.60 wt %. The groundmass consists of Na- and K-feldspar laths, clinopyroxene and magnetite microlites, and grains of chlorite, epidote, and hydrobiotite. All rocks contain accessory Cl-apatite. High-Ti basalts can be readily recognized among the main members of the shoshonitic series and differ from the volcanics of both series by their megaphyric texture, the lowest SiO_2 concentrations, and elevated contents of TiO_2, which is also typical of the pyroxene in these rocks. The cores of plagioclase phenocrysts are An_{96}. The rocks occur as relatively thin and strongly tectonized dikes within the trachybasalt succession and sills in the layered mudstone sequence. The contacts between the dikes and lavas are diffuse. The latites are noted for the phenocrystic assemblage of orthoclase and biotite and for elevated amounts of plagioclase among phenocrysts and feldspars among microlites. The porphyritic pyroxenites are made up of diopside phenocrysts in a diopside–magnetite matrix, whose interstices are filled with an albite–epidote–chlorite aggregate.

The high-Ti basalts contain occasional grains of Fe-rich orthopyroxene ($Wo_2En_{59-60}Fs_{38-39}$), and the trachybasalts have single grains of Cr-spinel (Cr_2O_3 = 49–51 wt %). In addition, the trachybasalts and pyroxenite contain diopside enclaves with inclusions of grossular (Flerov and Seliverstov, 1999).

The plagioclase-free potassic alkaline series includes absarokite flows; dikes and sills of shonkinites, leucite-bearing analcime shonkinite porphyries; subvolcanic bodies of shonkinites; and sills of orthoclase pyroxenites. Rocks of this series contain no plagioclase, and its clinopyroxene phenocrysts have the composition $Wo_{45-48.5}En_{39-47}Fs_{4-19}$, K_{mg} = 65–90, and Cr_2O_3 = 0–0.45 wt %. The absarokites consist of salite and, more rarely, magnetite phenocrysts and a groundmass with microlites of clinopyroxene, orthoclase, magnetite, and, more rarely, biotite. The mineralogy of the shonkinites and shonkinite porphyries is similar to that of the absarokites. Similarly to the latter rocks, the shonkinites and shonkinite porphyries are highly crys-

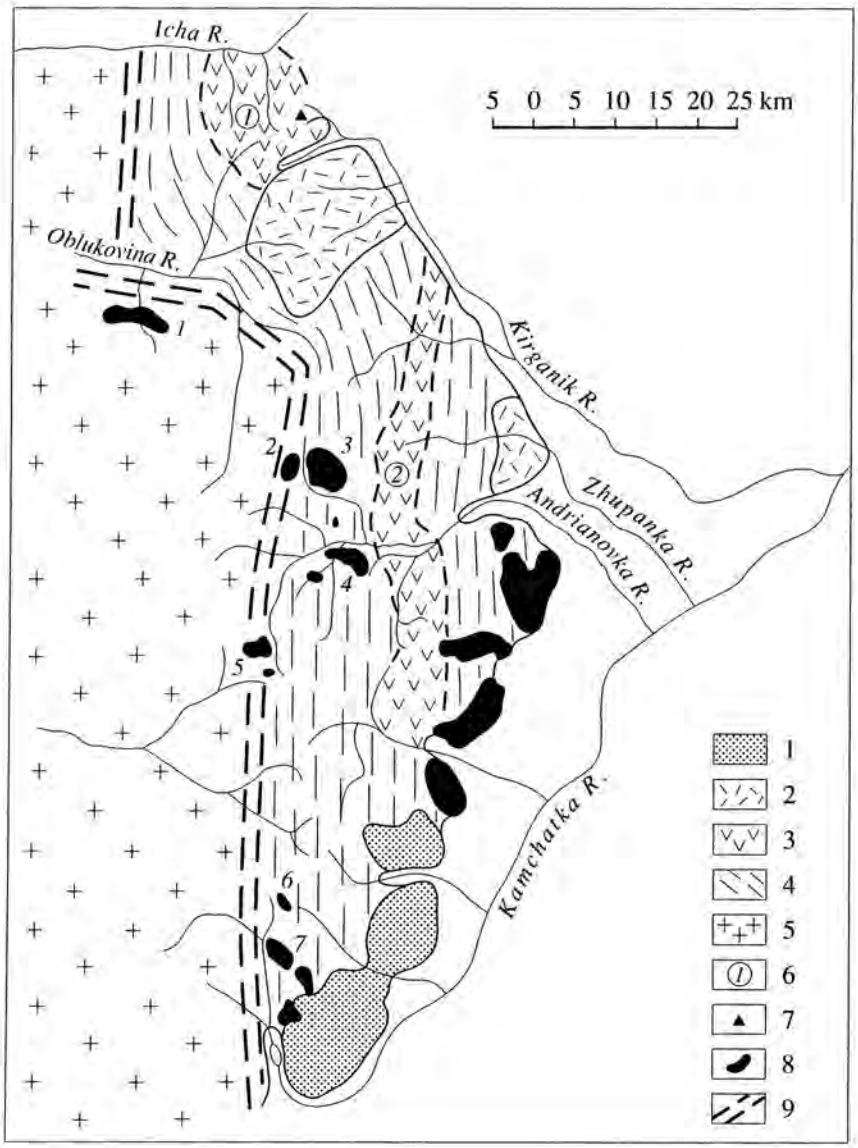

Fig. 1. Schematic map of Late Cretaceous–Paleogene rocks of the potassic alkaline association in central Kamchatka.
(1) Early Quaternary basalts; (2) Neogene volcanic rocks; (3) Late Cretaceous–Paleogene volcanic rocks of the Kirganik Formation; (4) Late Cretaceous volcano-sedimentary rocks of the Irunei Formation; (5) Paleozoic crystalline schists and gneisses of the Sredinnyi Massif; (6) study areas of volcanic rocks: areas of (*1*) the Kirganik, Saranskaya, Chengnuta, and Bogdanovskaya rivers, (*2*) Zhupanka and Andrianovka rivers; (7) field of potassic metasomatic rocks at the Sukhoe Ozero deposit; (8) massifs of the intrusive complex: (*1*) Filippa River pyroxenite, (*2*) Evseichikha River pyroxenite, (*3*) Evseichikha River gabbro–syenite, (*4*) Srednyaya Andrianovka River gabbro, (*5*) Levaya Andrianovka River pyroxenite–syenite and syenite, (*6*) Kunch River dunite–pyroxenite–monzonite, (*7*) Ozernaya Kamchatka River gabbro–monzonite; (9) fault zones.

talline (up to holocrystalline). Holocrystalline varieties include epileucitic shonkinites of subvolcanic bodies, which additionally contain epileucite and hastingsite phenocrysts. The phenocrysts of the leucite-bearing analcime shonkinite porphyries consist of analcime (pseudomorphs after leucite), salite, magnetite, and diopside. The pyroxene was determined to contain crystalline leucite inclusions and polycomponent melt and gas–melt inclusions rich in K. The groundmass is cryptocrystalline and consists of devitrified glass with numerous analcime rosettes, and microlites of clinopyroxene, magnetite, potassic feldspar, and biotite (Flerov *et al.*, 1998). The orthoclase pyroxenite contains clinopyroxene (85–90 vol %) and magnetite. Interstices are filled with aggregates of orthoclase, biotite, and magnetite. All rock types contain accessory Cl-apatite.

It should be mentioned that the classification of the rocks into series in accordance with the presence or absence of plagioclase is confirmed by the composition of the clinopyroxene, which displays distinct compositional trends in rocks of the shoshonitic and potassic alkaline series (Flerov and Seliverstov, 1999).

The close spatial and temporal relations between volcanics of the shoshonitic and potassic alkaline series, particularly their modal composition, confirm petrogenetic links between the volcanics of these series (Flerov and Koloskov, 1976; Flerov and Seliverstov, 1999). The aforementioned researchers admit that the diversity of rocks of the two series was caused by crystallization differentiation with clinopyroxene (and, perhaps, olivine) fractionation, potassium addition into the melts of the potassic alkaline series by transmagmatic fluid flows, and the mixing between derivatives of subalkaline and alkaline magmas.

The dunites are commonly monomineralic olivine (Fo_{85-89}) rocks, although some varieties contain up to 5 vol % diopside ($Wo_{47-50}En_{46-48}Fs_{4-5}$, K_{mg} = 89–92, and Cr_2O_3 = 0.13–0.53 wt %). An ubiquitous accessory mineral is Cr-spinel (Cr_2O_3 = 17–38 wt %). Fractures and interstices contain newly formed phlogopite, often in association with apatite.

The pyroxenites often contain magnetite (up to 5–10 vol %), biotite or phlogopite, and, sometimes, olivine (Fo_{83-84}, up to 10 vol %). The clinopyroxene composes a continuous series from diopside ($Wo_{48-50}En_{45-47}Fs_{5-7}$, K_{mg} = 86–90) to salite ($Wo_{49-51}En_{33-40}Fs_{10-16}$, K_{mg} = 70–80). The rocks of pyroxenite massifs along the Evseichikha and Filippa rivers are noted for elevated contents of magnetite (up to 20 vol %), which crystallizes in interstices and develops in the form of sideronitic textures. The rocks are often altered by hydrothermal and metasomatic processes.

The gabbro are biotite or, rarely, amphibole–biotite rocks; some varieties are gabbro-pyroxenite or melanocratic, leucocratic, and orthoclase-bearing derivatives. The modal composition of the rocks varies as follows (vol %): pyroxene 30–60, plagioclase 25–60, magnetite 5–15, and biotite 5–15. There are melanocratic and leucocratic varieties. The compositions of clinopyroxene and plagioclase vary over the intervals $Wo_{44-49}En_{38-42}Fs_{11-14}$, K_{mg} = 72–78, and An_{31-66}. The rocks occasionally contain single grains of olivine and orthopyroxene ($Wo_3En_{58-64}Fs_{33-39}$, K_{mg} = 64–66) and, always, accessory Cl-apatite.

The syenites and quartz syenites has the following modal composition (vol %): plagioclase 20–35, orthoclase 45–50, hornblende 10–15, quartz 5–15, biotite 5, and magnetite 5. The monzonites are represented by amphibole and quartz–amphibole varieties and contain (vol %): plagioclase 25–40, orthoclase 25–40, hornblende up to 40, magnetite 5 and biotite, quartz, and clinopyroxene account for 5 vol % each. All rocks contain accessory apatite, sphene, and, more rarely, ilmenite and zircon. The pyroxene has the composition $Wo_{46-50}En_{36-39}Fs_{12-16}$, K_{mg} = 71–75; plagioclase from the syenites and monzonites is An_{22-53} and An_{43-59}, respectively.

Clinopyroxene from rocks of different intrusive phases differs in composition, as is seen, for example, in *En–Wo–Fs* and element–K_{mg} plots [see Figs. 3 and 4 in (Flerov and Seliverstov, 1999)], in which the trends for pyroxene from the pyroxenites, gabbro, and syenites are differently directed and subparallel. These compositional trends of pyroxene and the fact that the massifs contain early intrusive phases with rocks that compose differentiation sequences with other compositional trends of their pyroxenes (an increase in the ferrosilite concentration) suggest the gravitational fractionation of pyroxenes and olivine during the crystallization of melts in intrusive chambers. This mechanism could also participate in magma differentiation at deeper levels (in intermediate chambers).

Of course, the composition of clinopyroxene from volcanic and intrusive rocks reflects different *P–T* conditions of their crystallization in magmatic systems. However, there are principal similarities between the crystallization schemes of this mineral in rocks of similar silicity in the trachybasalt–latite and gabbro–syenite successions. Although the compositions of salite from the trachybasalt and latite and from the gabbro and syenite compose distinct data-point swarms, the compositional trends of the pyroxenes are comparable: the trend for the former rock pair is defined by the composition $Wo_{45-49}En_{34-43}Fs_{12-17}$, and this compositional range for the latter pair is $Wo_{44-50}En_{36-42}Fs_{11-16}$. Furthermore, salite from the latites and syenites of the volcanic and intrusive complexes, respectively, are clearly different from the pyroxenes of all other rock types by K_{mg} and the concentrations of Al, Ti, and Al(IV) (Flerov and Seliverstov, 1999). This provides an argument for the comagmatic nature of the melts parental for these volcanic and intrusive rocks.

GEOCHEMISTRY

Let us discuss the composition of the rocks (Tables 1 and 2). In constructing the variation diagrams, we used previously published (Flerov and Koloskov, 1976; Fedorov and Dubik, 1990; *Geokhimicheskaya tipizatsiya...*, 1990; Flerov and Seliverstov, 1999) and newly obtained data.

In ($Na_2O + K_2O$) vs. SiO_2 (Fig. 2) and K_2O vs. SiO_2 (Fig. 3) variation diagrams, the rocks of the volcanic and intrusive complexes show a common tendency of positive correlations. The volcanics of both the shoshonitic and the potassic alkaline series compose continuous sequences from basalt (absarokite) to trachyandesite and latite (shonkinite), and practically all rocks of both series are plotted within the field for the shonkinite series (Peccerillo and Taylor, 1976) in a K_2O–SiO_2 plot (Fig. 3) and within the field for alkaline rocks in a ($Na_2O + K_2O$)–SiO_2 plot (Fig. 2). In the plots, the rocks compose two distinct trends. One of them is defined by rocks of the alkaline series and is characterized by a strong potassium enrichment at an insignificant increase in the silica concentration. These rocks are also characterized by elevated phosphorus concentrations. The other trend, which is defined by rocks of the shoshonitic series, is inclined less steeply. The

Table 2. Representative analyses of potassic plutonic rocks from central Kamchatka

Component	K60-5	K60-6	K60-1	K60-8	3015-1	3001	K67-1	3660-2	3439
	1	2	3	4	5	6	7	8	9
SiO_2	37.30	38.30	40.20	45.60	49.06	53.68	36.50	44.40	48.91
TiO_2	0.00	0.00	0.00	0.60	0.16	0.13	1.03	0.57	0.90
Al_2O_3	0.20	0.10	0.30	5.30	1.39	0.83	4.79	8.54	6.27
Fe_2O_3	–	–	–	–	3.82	0.49	14.48	4.70	2.37
FeO	11.60	12.20	14.00	11.00	4.32	2.82	8.81	6.95	3.93
MnO	0.20	0.20	0.30	0.20	0.12	0.10	0.25	0.22	0.12
MgO	41.60	45.00	43.10	14.70	20.76	17.01	11.24	14.18	13.91
CaO	1.20	0.20	1.90	18.10	15.10	23.67	15.58	16.16	22.27
Na_2O	0.00	0.00	0.00	0.40	0.22	0.24	0.24	0.44	0.46
K_2O	0.00	0.00	0.00	2.20	0.04	0.11	1.66	0.54	0.17
P_2O_5	0.00	0.00	0.00	0.70	0.04	0.02	1.96	0.43	0.04
LOI	–	–	–	–	4.65	–	–	3.34	–
Total	92.10	96.00	99.80	98.80	99.62	99.08	96.54	100.47	99.35
Cr	1714	2606	2725	740	703	1616	118	599	1870
Ni	1246	2191	1220	205	415	147	76	214	118
Co	133	142	140	56	76	29	68	62	38
Sc	9	5	11	73	38	53	59	53	102
V	9	13	22	302	61	59	578	359	275
Cs	0.05	0.02	0.02	1.04	0.20	0.10	2.70	1.40	0.10
Rb	0.93	0.50	0.55	52	2	4	46	15	2
Sr	2.43	0.98	5.38	72	75	40	152	235	72
Ba	22	8	13	450	80	46	209	140	49
Be	0.02	0.02	0.02	0.04	–	–	0.10	–	0.20
Y	–	–	–	9	2	2	16	11	9
Zr	9	8	9	15	10	12	17	18	20
Hf	0.02	0.01	0.02	0.39	0.10	0.03	0.50	0.50	0.53
Ta	0.01		0.03	0.05	–	–	–	–	–
Nb	0.00	0.10	0.00	0.60	0.20	0.10	0.50	0.20	0.80
U	0.02	0.01	–	0.02	–	–	–	–	–
Th	0.02	0.01	0.10	0.05	0.10	–	0.30	–	–
La	0.05	0.01	0.05	1.46	0.40	0.20	2.60	1.60	0.80
Ce	0.01	–	0.13	3.60	1.10	0.70	8.00	4.80	2.50
Pr	0.01	–	0.03	0.69	0.20	0.10	1.50	0.90	0.50
Nd	0.09	0.04	0.19	3.92	1.15	0.95	8.40	5.35	3.50
Sm	0.04	0.03	0.07	1.59	0.40	0.40	3.00	1.95	1.40
Eu	0.02	0.01	0.03	0.58	0.10	0.10	1.00	0.60	1.50
Gd	0.05	0.02	0.10	1.62	0.45	0.45	3.35	2.20	1.60
Tb	0.01	0.01	0.02	0.30	0.08	0.08	0.57	0.38	0.30
Dy	0.06	0.03	0.09	1.72	0.45	0.45	3.00	2.35	1.70
Ho	0.01	0.01	0.02	0.24	0.09	0.08	0.57	0.47	0.31
Er	0.05	0.02	0.06	0.91	0.20	0.20	1.50	1.30	0.80
Tm	0.01	0.01	0.01	0.13	0.03	0.03	0.20	0.18	0.11
Yb	0.04	0.04	0.07	0.77	0.20	0.20	1.20	1.10	0.70
Lu	0.01	–	0.01	0.12	0.03	0.02	0.17	0.16	0.09

Table 2. (Contd.)

Component	K3624-3	3400	K60	K3677	3103-2	3448	3402-2	2047v	3447
	10	11	12	13	14	15	16	17	18
SiO_2	46.79	45.43	54.00	51.58	56.06	50.42	58.62	59.22	62.23
TiO_2	0.82	0.79	0.60	0.80	0.54	0.68	0.47	0.42	0.37
Al_2O_3	14.57	14.17	18.10	16.29	16.22	13.25	16.17	17.19	15.40
Fe_2O_3	4.09	5.95	–	3.51	2.26	4.77	3.52	2.00	2.33
FeO	6.24	6.09	7.90	4.86	4.69	6.27	3.00	2.77	2.77
MnO	0.21	0.25	0.20	0.18	0.17	0.22	0.14	0.14	0.12
MgO	7.73	6.94	3.60	4.85	3.62	6.65	2.65	1.72	2.54
CaO	12.09	12.74	7.70	9.09	6.51	10.50	5.11	4.29	4.64
Na_2O	1.94	2.29	3.10	2.62	2.78	2.42	3.82	3.81	3.66
K_2O	1.68	1.10	3.20	3.66	4.61	2.13	5.04	7.16	4.63
P_2O_5	0.59	0.54	0.50	0.55	0.41	0.61	0.32	0.24	0.23
LOI	2.46	–	–	1.74	–	–	–	–	–
Total	99.21	96.29	98.90	99.73	97.87	97.92	98.86	98.96	98.92
Cr	165	114	70	62	55	146	37	28	56
Ni	50	36	74	22	21	39	12	13	16
Co	42	39	22	25	24	40	17	12	15
Sc	42	39	31	32	25	36	14	12	16
V	388	360	285	323	217	301	166	178	127
Cs	1.10	0.50	0.44	1.70	0.60	0.50	0.60	1.30	1.10
Rb	28	22	54	69	87	39	79	131	77
Sr	405	1108	492	314	417	799	847	797	536
Ba	382	478	600	556	1109	487	911	437	545
Be	0.30	0.50	0.79	0.50	0.70	0.90	1.40	1.50	1.20
Y	16	18	18	18	24	19	18	17	26
Zr	22	15	13	51	87	35	72	41	93
Hf	0.80	0.70	0.87	0.73	1.56	1.23	1.50	1.13	0.80
Ta	0.10	0.10	0.21	0.40	0.50	0.20	0.30	0.40	0.40
Nb	1.80	0.80	4.30	3.80	4.10	1.60	2.30	2.60	1.40
U	0.10	0.10	0.30	0.30	0.40	0.60	1.10	0.60	0.50
Th	0.30	0.30	0.79	0.70	1.20	1.50	2.10	1.20	1.70
La	4.50	7.90	7.15	5.30	7.20	12.20	12.20	7.70	8.80
Ce	11.00	19.80	14.89	12.90	18.30	26.90	27.30	17.90	19.10
Pr	1.70	3.20	1.99	1.90	2.60	3.90	4.00	2.60	2.60
Nd	9.20	16.50	9.05	9.45	13.20	17.80	17.85	11.85	11.35
Sm	2.80	4.30	2.81	2.85	4.10	4.70	4.40	3.30	2.75
Eu	0.95	1.45	0.94	1.00	1.25	1.30	1.30	1.00	0.80
Gd	3.00	4.00	2.77	3.00	4.10	4.10	3.75	3.05	2.35
Tb	0.55	0.69	0.48	0.53	0.74	0.67	0.61	0.51	0.40
Dy	3.05	3.65	2.80	3.25	4.60	3.90	3.35	3.10	2.20
Ho	0.63	0.72	0.59	0.60	0.94	0.76	0.65	0.62	0.44
Er	1.70	2.00	1.80	2.00	2.90	2.00	1.90	1.90	1.30
Tm	0.26	0.31	0.29	0.30	0.41	0.31	0.29	0.30	0.20
Yb	1.55	1.75	1.77	1.90	2.70	2.00	1.80	1.80	1.35
Lu	0.23	0.25	0.27	0.28	0.39	0.30	0.27	0.28	0.20

Note: (1–3) Dunite, (4–9) pyroxenite, (10, 11) gabbro, (12–15) monzonite, (16–18) syenite. Massifs near rivers: (1–4, 12) Kunch, (5, 6, 17) Levaya Andrianovka, (7) Filippa, (15, 18) Evseichikha, (8, 10, 13, 14) Ozernaya Kamchatka, (11, 16) Srednyaya Andrianovka, (9) xenolith from lava breccia at the Saranskaya River. Dashes mean not determined.

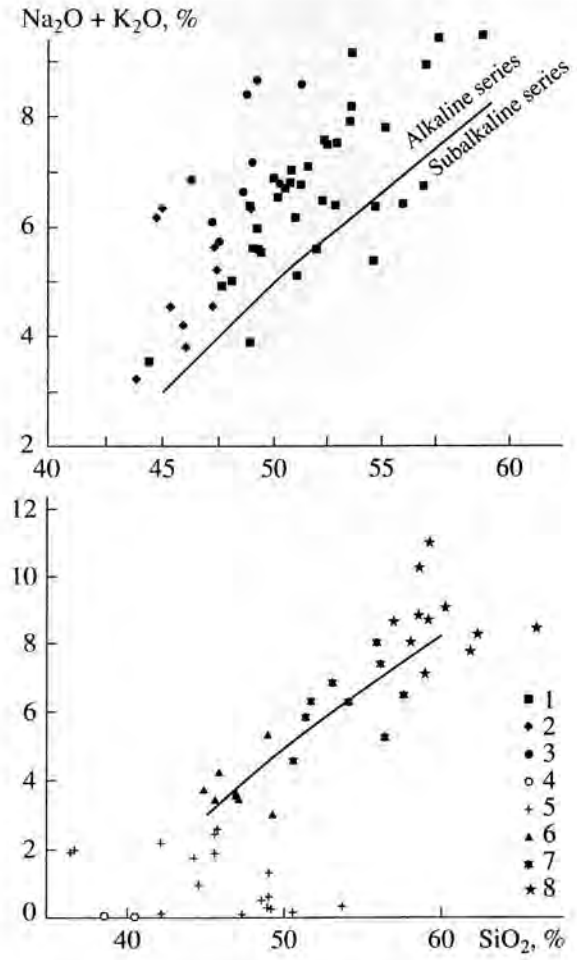

Fig. 2. SiO_2–($Na_2O + K_2O$) plot for Late Cretaceous–Paleogene magmatic rocks in central Kamchatka.

Volcanic complex: (1, 2) shoshonitic series: (1) basalts, trachybasalts, latites, essexites, and pyroxenites, (2) high-Ti basalts; (3) potassic alkaline basaltoid series. Intrusive complexes: (4) dunites; (5) pyroxenites; (6) gabbro; (7) monzonites; (8) syenites. The dividing line is after (Irvine and Baragar, 1971).

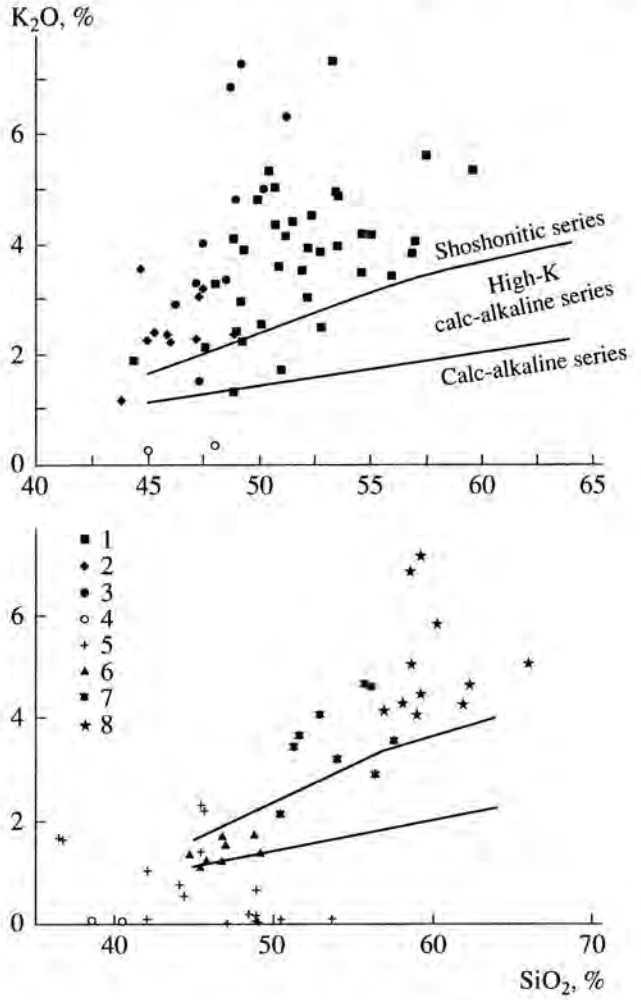

Fig. 3. SiO_2–K_2O plot for Late Cretaceous–Paleogene magmatic rocks in central Kamchatka.

See Fig. 2 for notation. The dividing line is after (Peccerillo and Taylor, 1976).

K_2O/Na_2O ratio varies from 0.7–0.8 to 2.5 in rocks of the shoshonitic series and attains 5 in rocks of the potassic alkaline series. In terms of K concentration, rocks of the intrusive complex vary (Fig. 3) from nearly potassium-free dunites and some pyroxenites to potassic gabbro, pyroxenites, and syenites. All rocks of both complexes are low in TiO_2. The only exception is a group of high-Ti basalts (up to 1.6–1.7 wt % TiO_2, Table 1). Given the fact that pyroxene from these rocks is also high in Ti (Flerov and Seliverstov, 1999), it is reasonable to suggest that the parental melts of these rocks could be enriched in this element.

The compositional similarities and differences between these complexes are pronounced most clearly in spider diagrams (Fig. 4) in terms of the concentrations of incompatible elements normalized to the primitive mantle (Sun and McDonough, 1989). The positive anomalies at LILE and minima at HFSE, particularly the strong Nb–Ta anomalies, point, on the one hand, to similarities between the rocks (except their K and P concentrations) and, on the other hand, to the subduction-related genesis of both complexes (Gill and Whelan, 1989). The compositional similarities between the rocks of the shoshonitic and potassic alkaline series of the volcanic and intrusive complexes become even more conspicuous when their element ratios are analyzed. As is seen from Table 3 and Fig. 4, the element ratios of the rocks can be subdivided into three groups: lower than in the primitive mantle (Th/U, Ti/P, Nb/Ta, and Nb/Th), close to those in the primitive mantle (Ti/Zr and Zr/Y), and higher than in the primitive mantle (ratios of alkalis, alkali earths, rare earths, Ba/Nb, and La/Ta). The ratios of most elements vary insignifi-

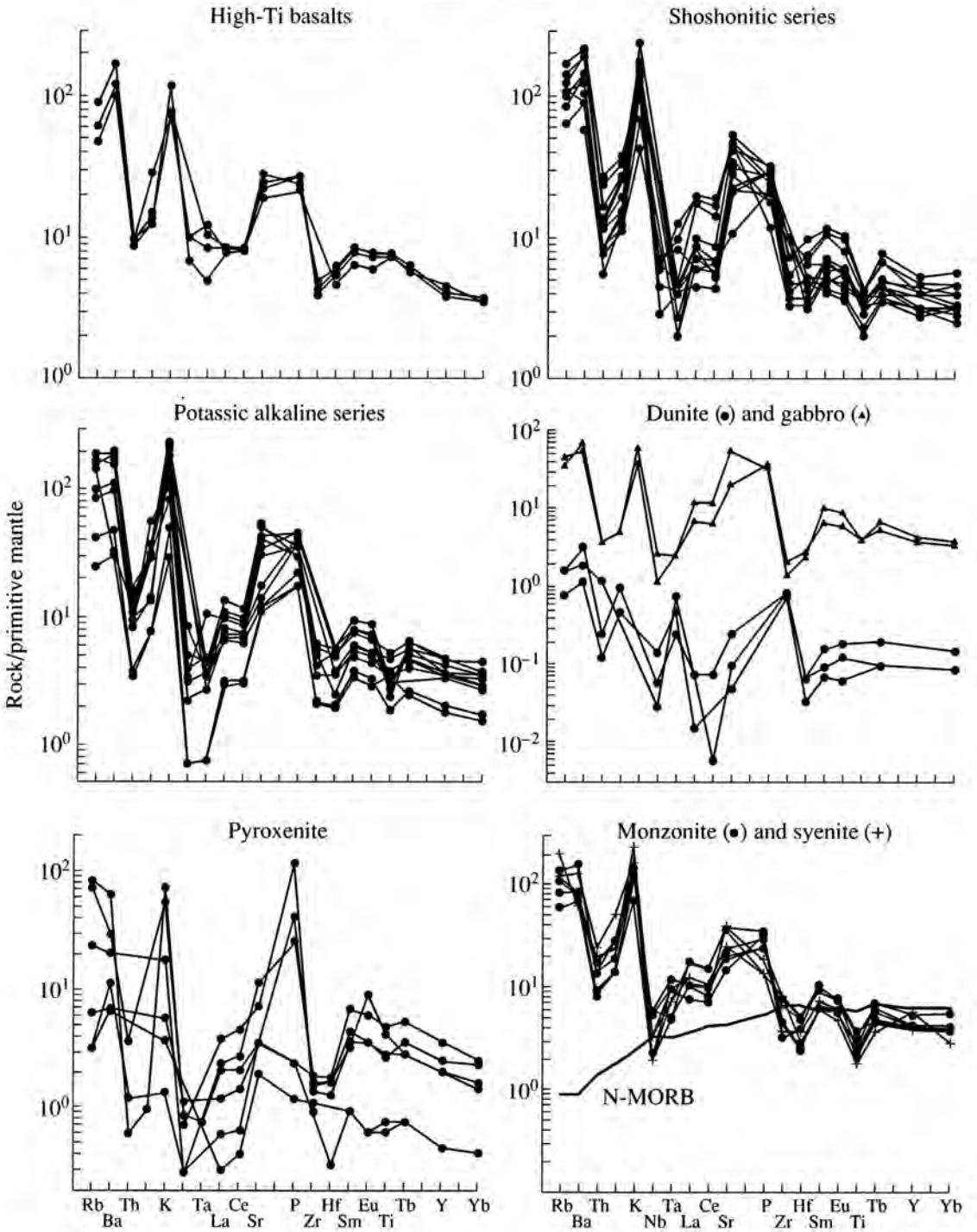

Fig. 4. Plots of incompatible elements, normalized to the primitive mantle, for Late Cretaceous–Paleogene magmatic rocks in central Kamchatka.

N-MORB values are after (Sun and McDonough, 1989). The incompatible-element concentrations in basalts are normalized to the primitive mantle (after Sun and McDonough, 1989).

cantly in rocks of both the volcanic and intrusive complexes.

It should be taken into consideration that the comagmatic character of rocks of the alkaline association in central Kamchatka did not result from the differentiation of a single geologic body but was caused by a systematic combination of and genetic links between rocks of different compositions and facies affinities (Koloskov, 1982; Flerov and Koloskov, 1976). In the recognized successions gabbro–syenite (monzonite)

Table 3. Element ratios in rocks of the volcanic and intrusive complexes

Rock	K/Rb	Ba/Sr	Rb/Cs	Th/U	Nb/Ta	Zr/Nb	Ti/Zr
High-Ti basalt	470–480	1.6–2.5	20–30	1.3–2.7	14–24	6.6–9	180–220
Trachybasalt	350–500	0.5–3.1	28–78	2–2.9	8–26	10–22	30–120
Latite	660–670	1.1–1.4	111	2.2–2.7	12	27	49
Pyroxenite	–	1.8	–	2.9	–	–	
Absarokite	230–620	0.8–2.2	–	0.9–2.9	43	9	56–108
Shonkinite	510–520	0.9–1.5	60–90	1.8–2.3	14–14.6	16.4	140
Lc shonkinite	500–540	1.2–1.7	170	0.7–2	6–20	20–27	47–115
Ort pyroxenite	460.00	1.35	21.1	2.00	17.0	46.00	99.04
Dunite	–	2.6–11	20–50	1	0.7–5	80–450	–
Pyroxenite	170–830	0.6–10.5	10–50	2.5	20	25–120	60–300
Gabbro	420–500	0.4–1.2	25–120	2.6–3	8–20	10–19	80–315
Monzonite	440–450	0.6–2.7	80–145	2.5–3	8–8.2	21–22	37–117
Syenite	450–530	0.5–1.1	70–130	1.9–3.4	3.5–7.7	15–67	24–60
Primitive mantle	394	0.33	19.8	4	17.4	15.7	116
N-MORB	1070	0.07	80	2.6	17.7	31.8	103

Rock	Zr/Y	La/Sm	La/Yb	Ba/Nb	Ti/P	Nb/Th	La/Ta
High-Ti basalt	2.5–2.7	0.9–1.3	1.9–2.2	100–240	3.7–4.8	6.2–9.6	14–28
Trachybasalt	2.6–6.2	1.1–1.6	1.8–3.9	200–460	1.2–4.9	2–4.2	12–29
Latite	4.4	1–1.3	1.3–1.5	320	1.2–1.4	3.1	2.8–18
Pyroxenite		1.3	2.75		1.4	1.6	67
Absarokite	2.7–3.7	1–1.4	1.7–2.7	39	1.3–2.8	6	32
Shonkinite	2.3	0.8–1.3	1.4–2.8	280–500	0.8–2.2	1.8–4	23–48
Lc shonkinite	2.6–4.3	1.2–1.4	2.5–3.7	370–560	0.7–1.7	2–2.9	15–46
Ort pyroxenite	2.56	0.73	1.63	670.0	1.4	1.6	67
Dunite	–	0.2–0.8	0.2–0.8	80–650	–	0.2–2	1.7–5.2
Pyroxenite	1.1–6	0.3–0.6	0.7–1.4	400–750	0.6–7	1.6–2	48
Gabbro	0.8–2.4	1–1.6	1.9–3	140–600	1.2–1.6	2.7–6	35–79
Monzonite	1.8–3.6	1–1.6	1.7–4	270–300	1.2–1.4	1.7–3.4	7–14
Syenite	2.4–4	1.4–1.9	2.8–4.5	170–390	1.6–1.9	0.9–2.1	19–22
Primitive mantle	2.5	0.95	0.92	9.8	13.7	8.4	16.8
N-MORB	2.6	0.58	0.54	2.7	14.9	19.4	18.9

Note: High-Ti basalt is basalt with an elevated titania concentration; *Lc*–leucite, *Ort*–orthoclase; element ratios in the primitive mantle and N-MORB are given after (Sun and McDonough, 1989).

and trachybasalt (basalt)–latite, all rocks are characterized by apparently elevated concentrations of K, similar isotopic Sr and Nd compositions (Table 4, Fig. 5), and similar intervals of trace-element ratios (Table 3) and, therefore, can be regarded as members of a single comagmatic volcano–plutonic association. The high trace-element concentrations of the rocks are clearly correlated with the general chemical trend of the rocks. Figure 6 demonstrates the distribution of some incompatible elements relative to Ce. The linear character of the distribution of elements in rocks of distinct facies affinities and chemical compositions provide further evidence for their common genesis as a consequence of differentiation of a primary magma.

The distribution of REE in the rocks of both complexes is weakly fractionated: the normalized HREE concentrations are 2–5 times lower than in MORB (Fig. 7). The orthoclase pyroxenites are even more strongly depleted in HREE and can be probably assigned to cumulates. This is also confirmed by mineralogical evidence (Flerov and Seliverstov, 1999). Shoshonitic-series rocks with similar REE patterns are known to occur among the lavas of Kekuknai volcano in Kamchatka (Volynets *et al.*, 1986) and Viti Levu

Table 4. Isotopic data on clinopyroxene and syenite from the Late Cretaceous–Paleogene alkaline rock association in central Kamchatka

No.	$^{147}Sm/^{144}Nd$	$^{143}Nd/^{144}Nd$ (0)	$^{143}Nd/^{144}Nd$ (50)	ε^0	ε^t	$^{87}Rb/^{86}Sr$	$^{87}Sr/^{86}Sr$ (0)	$^{87}Sr/^{86}Sr$ (50)	ε^0	ε^t
1	–	–	–	–	–	0.1550	0.70383 ± 2	0.70372	–9.6	–10.3
2	0.25172 ± 6	0.513003 ± 8	0.512921	+7.1	+6.8	0.0404	0.70349 ± 2	0.70347	–14.3	–13.9
3	–	–	–	–	–	0.1337	0.70361 ± 2	0.70351	–12.7	–13.2
4	–	–	–	–	–	0.1594	0.70351 ± 2	0.70340	–14.0	–14.8
5	0.24858 ± 9	0.513013 ± 19	0.512932	+7.3	+7.0	0.1197	0.70365 ± 2	0.70356	–12.1	–12.5
6	0.23283 ± 4	0.513057 ± 6	0.512981	+8.2	+7.9	0.0919	0.70348	0.70341	–14.5	–14.6
7	0.25276 ± 5	0.513112 ± 9	0.513029	+9.2	+8.9	0.0514	0.70335 ± 2	0.70331	–16.4	–16.0
8	0.20693 ± 10	0.513003 ± 28	0.512935	+7.1	+7.0	0.0063	0.70344 ± 1	0.70344	–15.0	–14.3
9	0.21874 ± 5	0.513080 ± 9	0.513008	+8.6	+8.5	0.0492	0.70331 ± 2	0.70327	–17.0	–16.6
10	0.19873 ± 7	0.513098 ± 7	0.513033	+9.0	+9.0	0.0161	0.70331 ± 2	0.70330	–17.0	–16.3
11	–	–	–	–	–	0.0656	0.70337 ± 2	0.70333	–16.0	–15.8
12	0.21865 ± 5	0.513043 ± 10	0.512972	+7.9	+7.8	0.0539	0.70344 ± 2	0.70340	–15.0	–14.7
13	0.26531 ± 8	0.513028 ± 10	0.512941	+7.9	+7.2	0.0806	0.70378 ± 2	0.70372	–10.2	–10.2
14	–	–	–	–	–	0.0315	0.70360 ± 3	0.70358	–12.8	–12.2
15	0.22264 ± 4	0.512934 ± 8	0.512861	+5.8	+5.6	0.0252	0.70358 ± 2	0.70357	–13.0	–12.4
16	0.19968 ± 8	0.513062 ± 8	0.512997	+8.3	+8.3	0.0351	0.70338 ± 2	0.70336	–15.9	–15.4
17	0.16186 ± 8	0.513041 ± 7	0.512985	+7.9	+8.0	0.4673	0.70384 ± 3	0.70351	–9.4	–13.2
18	0.14113 ± 10	0.513021 ± 8	0.512975	+7.5	+7.8	0.3568	0.70361 ± 2	0.70336	–12.6	–15.3

Note: (1–16) Clinopyroxene. (1–8) Shoshonitic series: (1, 2) high-Ti basalt, (3–6) trachybasalt, (7) latite, (8) porphyritic pyroxenite; (9–12) potassic alkaline series: (9) absarokite, (10) epileucite shonkinite, (11) leucite-bearing analcime shonkinite porphyry, (12) orthoclase pyroxenite; (13–18) plutonic association: (13–15) pyroxenite, (16) gabbro, (17, 18) whole-rock syenite samples. Massifs near rivers: (13) Kunch, (14, 15, 17) Levaya Andrianovka, (16) Srednyaya Andrianovka, (18) Evseichikha. The isotopic composition of Samples 17 and 18 was analyzed after their treatment by 0.1 N HCl.

Island, Fiji (Gill, 1970). Such low HREE concentrations suggest a depleted source in the mantle wedge. The source was, perhaps, produced by the earlier melting of a source close to MORB during the within-plate rifting (Churikova *et al.*, 2000). The low isotopic ratios of Sr ($^{87}Sr/^{86}Sr$ = 0.703271–0.703512) and high isotopic ratios of Nd ($^{143}Nd/^{144}Nd$ = 0.51285–0.51303) in the lavas of both series are generally consistent with this conclusion (Table 4).

The data presented above on the distribution of major and trace elements in the lavas of the shoshonitic and potassic alkaline series and rocks of the intrusive complex suggest their origin from a single source.

DISCUSSION

Shoshonite lavas are known to be derivatives of fairly unusual island-arc magmas (Tsvetkov *et al.*, 1993), which are characterized, in addition to high concentrations of K, by high contents of LILE and lower concentrations of HFSE (LILE/HFSE > 1).

One of the key problems in the genesis of shoshonitic magmas is their high K concentrations. The K enrichment in island-arc magmas could be caused by several processes, both primary (deep-seated) and secondary (postmagmatic). The latter include hydrothermal reworking of the rocks. Evidence for the action of this process is provided, for example, by the extensive field of the Sukhoe Ozero hydrothermal–metasomatic deposit in the headwaters of the Kirganik River. The rocks of this deposit are typical metasomatics with large (up to 3–4 cm) crystals of potassic feldspar (Flerov and Koloskov, 1976). However, the genesis of such K-rich solution remains obscure and could be related to the regionally elevated K concentration in the rocks of this province.

The primary processes that could result in K enrichment in the rocks probably included the contamination of the primary basaltic melts by crustal material rich in lithophile elements; the enrichment of the source by K from the melted sediments in the subducted oceanic plate; the enrichment of the primary melts in light lithophile elements during the partial melting of the source material; the introduction of LILE as a result of primary melt interaction with fluid, which migrated from the dehydration zone of the subducted oceanic lithosphere; LILE inflow in response to the interaction of the primary melt with another melt that migrated from the melting zone of the subducted oceanic crust; the derivation of the magmas from a source in the enriched

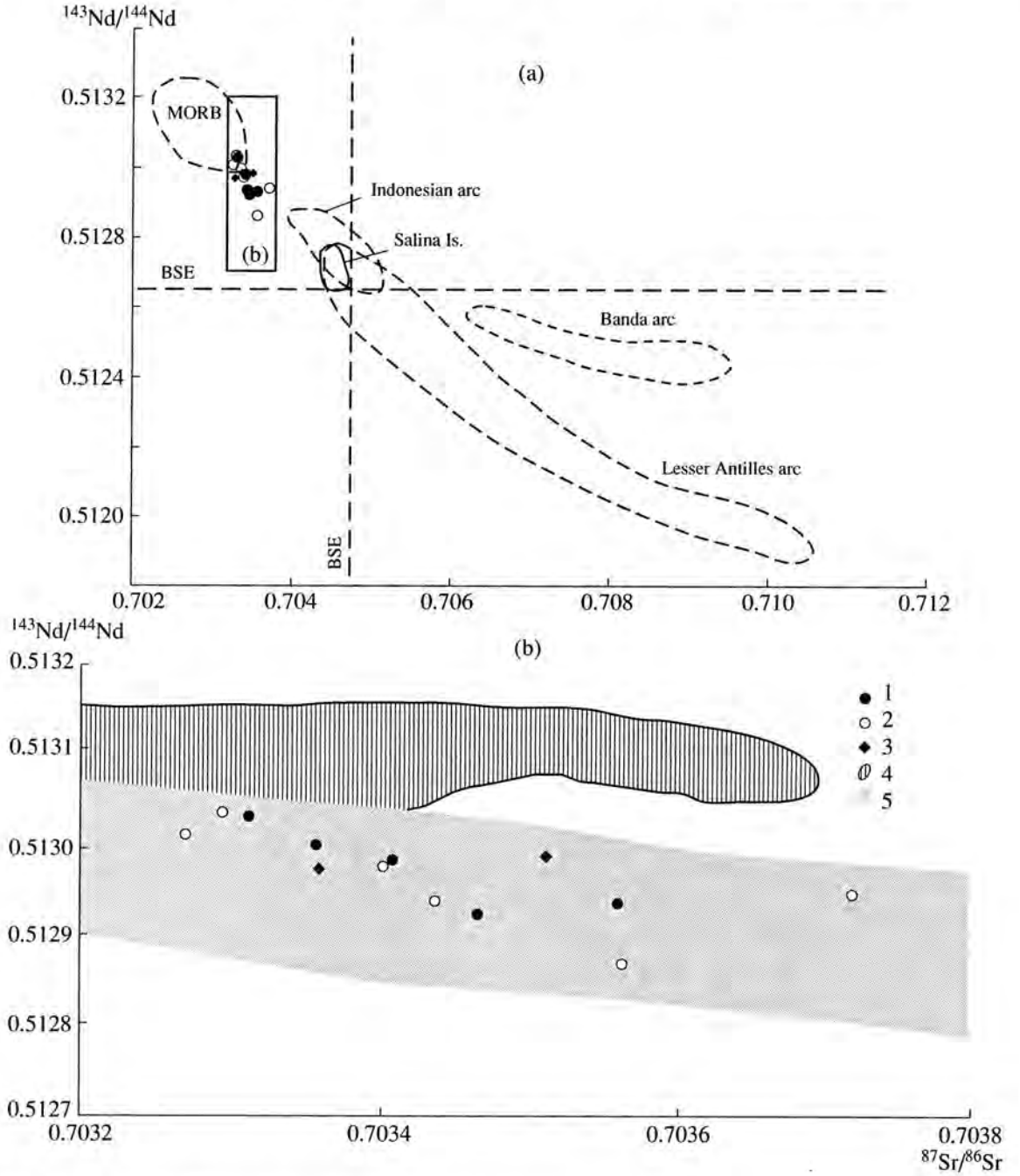

Fig. 5. $^{87}Sr/^{86}Sr$ vs. $^{143}Nd/^{144}Nd$ plot for clinopyroxene and syenites from central Kamchatka.

(1, 2) Isotopic composition of clinopyroxene from (1) shoshonitic and (2) potassic alkaline associations, including pyroxenites; (3) whole-rock isotopic composition of the syenites.

In the inset (b), (4, 5) isotopic compositions of basaltoids from Kamchatka: (4) island-arc and (5) within-plate geochemical types (Koloskov *et al.*, 2000). The compositional fields are given after: MORB (Hart, 1988); East Java, Indonesia (Edward *et al.*, 1994); Banda island arc (Whitford *et al.*, 1981); Lesser Antilles island arc (Davidson, 1986); Salina Island, Eolian island arc (Ellam *et al.*, 1989); BSE is the Bulk Silicate Earth.

mantle (under phlogopite control or other enrichment processes).

Inclusions of liquidus leucite (Flerov *et al.*, 1998) and K-rich melts in clinopyroxene from the shonkinite porphyry and orthoclase and biotite phenocrysts in the latites provide convincing evidence that the alkalinity of the primary magmas was potassic. At the same time, the wide variations in the K concentration of the trachybasalts (this phenomenon results in the shift of the data points of the rocks toward the compositional field of the

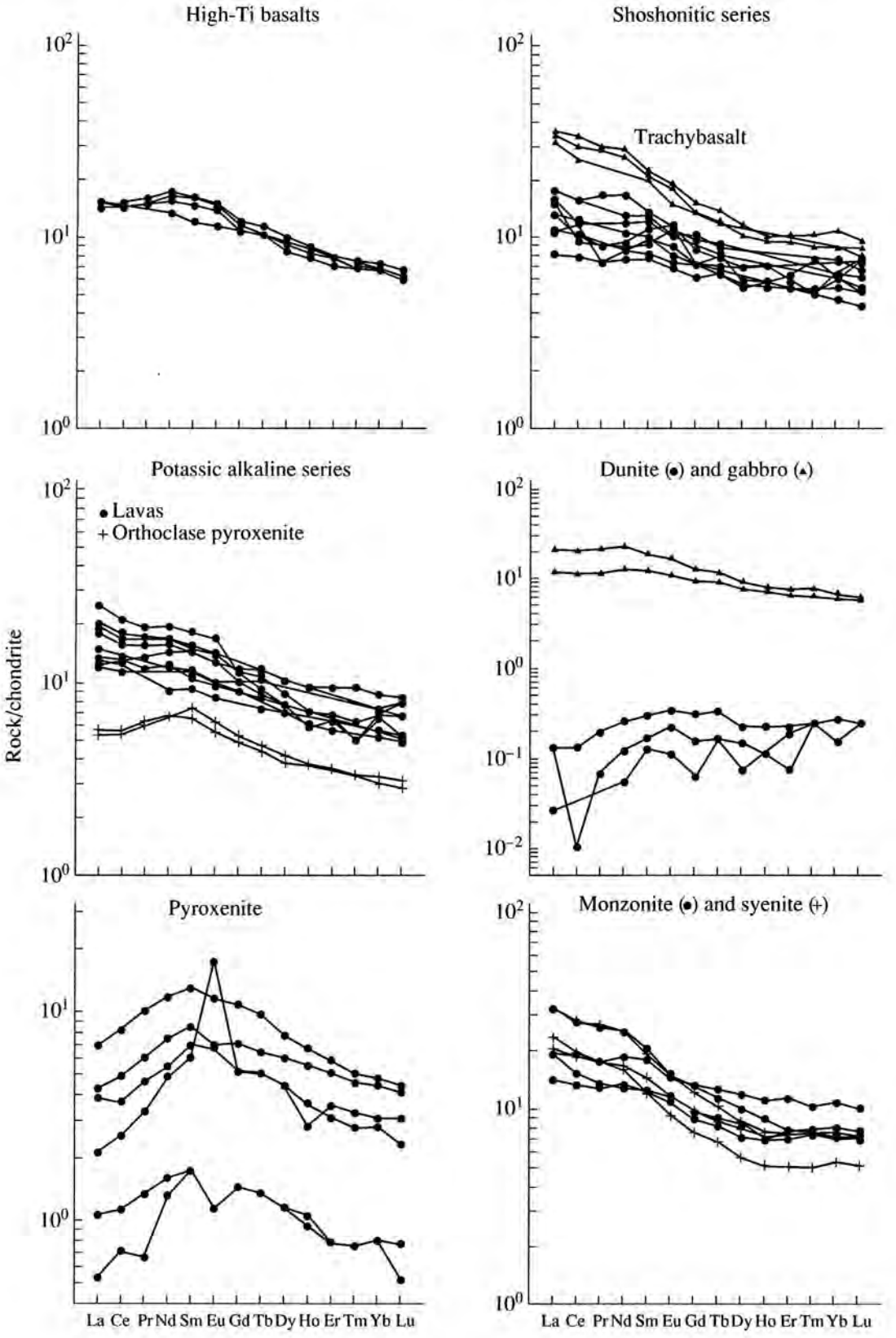

Fig. 6. Chondrite-normalized REE plots for Late Cretaceous–Paleogene magmatic rocks in central Kamchatka. The REE concentrations in basalts are normalized to chondrite (after Pallister and Knight, 1981).

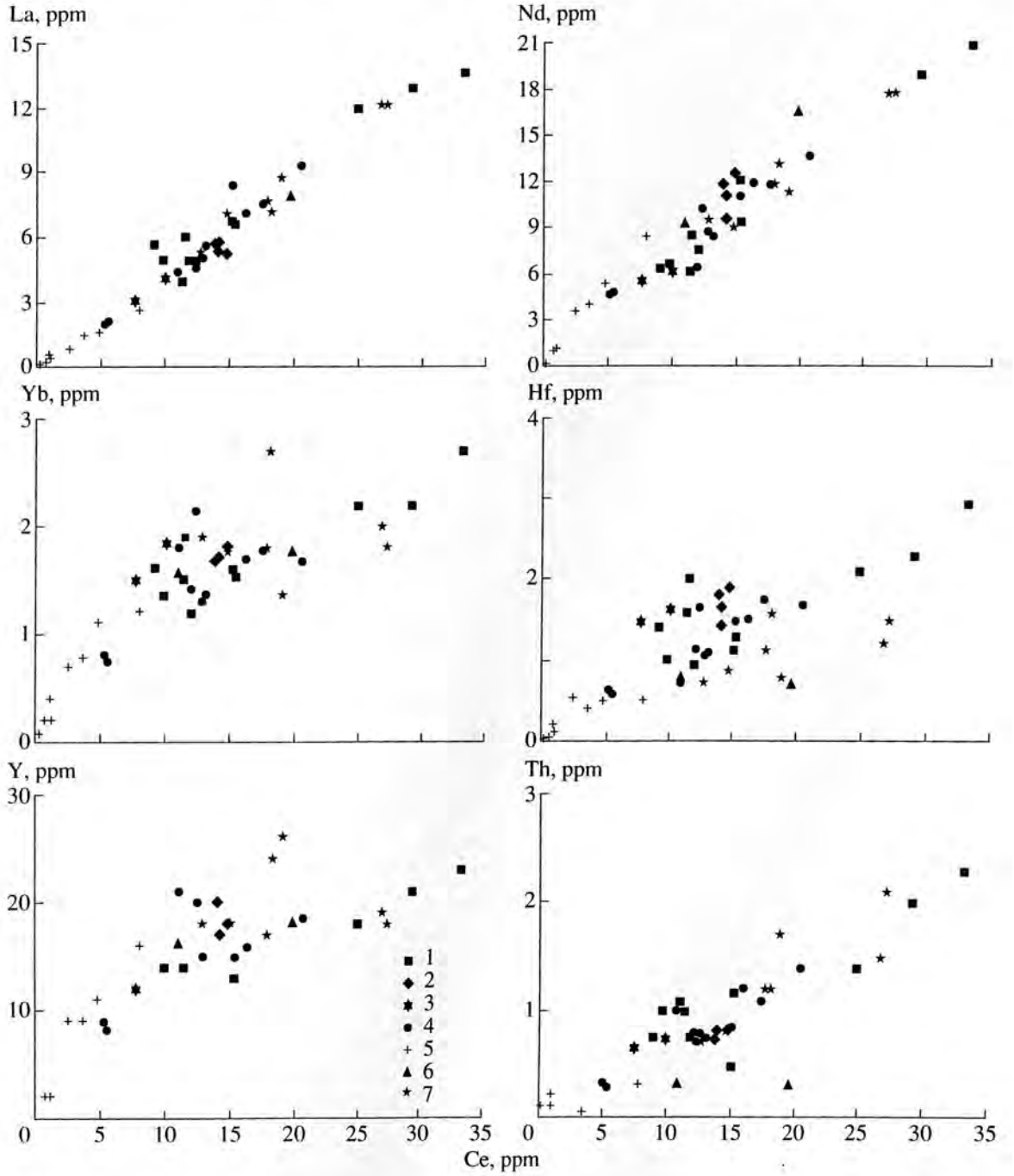

Fig. 7. Distribution of incompatible elements relative to Ce.
Volcanic complexes. (1–3) Shoshonitic series: (1) basalts, trachybasalts, latites, essexites, and pyroxenites, (2) high-Ti basalts, (3) latites; (4) potassic alkaline basaltoid series. Intrusive complex. (5) Dunites, pyroxenites; (6) gabbro; (7) syenites, monzonites.

potassic alkaline series in a K_2O vs. SiO_2 plot, see Fig. 3) do not exclude a possibility of the mixing of subalkaline and high-K alkaline melts and their later metasomatic recycling. This is also confirmed by data on the mineralogy of the volcanic rocks (Flerov and Seliverstov, 1999).

The high alkalinity of rocks of the shoshonitic series is usually explained by the contamination of the primary basaltic melts by crustal material (Kontak *et al.*, 1986). This hypothesis can be tested by analyzing the Sr and Nd isotopic compositions. As was mentioned above, the Sr isotopic ratios of the pyroxenes and rocks of the association vary from 0.70327 to 0.70358, and the Nd ratios range from 0.51285 to 0.51303 and do not notably differ in volcanics of different series. Analogous isotopic ratios are characteristic of the island-arc

mantle, a fact testifying to the mantle provenance of these rocks. Thus, the introduction of K and other LILE could not be caused by the addition of crustal material. However, the fact that the rocks of the shoshonitic series contain no orthopyroxene and grossular, which are xenogenic phases, suggests the partial contamination of the magmas by crustal material during their ascent to the surface. The Cr-spinel also provides evidence of mantle contamination by crustal material (Flerov and Seliverstov, 1999). Of course, this did not affect the results of the isotopic study, which were based on monomineralic separates of clinopyroxene phenocrysts.

The works of many researchers conducted over the past decade and devoted to the isotopic systematics of Pb and Be in the volcanics of Kamchatka and sedimentary rocks of the Pacific Plate (Kersting and Arculus, 1995; Volynets, 1994) have demonstrated that sediments played a very insignificant role during the origin of igneous rocks of Kamchatka. This means that the fluid that controlled the melting of the mantle material was more probably derived during the dehydration of material of the second oceanic-crust layer that from the sedimentary cover.

As is seen in the spidergrams (Fig. 4) the volcanics of the alkaline association in central Kamchatka are two and more times depleted in heavy trace elements compared with N-MORB, and, hence, the suggestion that they could have been derived from the enriched mantle is hardly realistic. As many other volcanic rocks in the Sredinnyi Range (Vinogradov *et al.*, 1986), these rocks were generated from a depleted source, which seem to have resulted from the earlier differentiation of a source similar to MORB. Direct calculations of the partial melting indicate that even a very low melting degree (<1%) of an enriched source could not give rise to rocks as strongly oversaturated in K, Ba, U, Rb, and other LILE. The rocks of the association normally have very high Ba/La ratios, which are appreciably larger than the values (80–90) used to characterize the subduction component of an island-arc environment in the mixing model (Lin *et al.*, 1989). This LILE enrichment could be related, first and foremost, to the addition of fluid (or melt), which was derived by the dehydration (or melting) of the subducted oceanic crust. To unambiguously resolve this problem, let us consider elements that behave differently in fluid and melt. These elements are, first of all, Nb, Ta, Hf, Zr, and Ti, because they are virtually immobile in fluid but are the first to pass into melt (as incompatible elements) during the melting of a plate. It can be seen from Fig. 4 that the rocks under consideration display a significant dispersion in all of these elements, probably, because of fractional crystallization. However, low concentrations of the aforementioned elements and high concentrations of K, Rb, Sr, Ba (as compared with their concentrations in a MORB source), and P provide evidence for the inflow of fluid rather than the addition of the melted oceanic crust to the mantle source.

Another possible mechanism of the enrichment of the source in K could be the melting of primary mantle material that contained phlogopite during this process. However, melting of this type should have resulted in the enrichment of the rock not only in LILE and K but also in Nb, Ti, and Zr, i.e., elements at which the spidergrams have negative anomalies (Fig. 4).

It can also be hypothesized that the asthenospheric mantle contained veinlets of spinel- and garnet-bearing pyroxenite, which were later metasomatized by fluids from the subducted plate at depths more than 60 km, and this led to the development of hornblende (amphibole) veinlets with or without phlogopite (Irving, 1980). These fluids enriched the mantle in LILE and, thus, increased the Ba/La ratio of the source. Convective flows within the mantle wedge displaced this mantle to depths of approximately 90 km, into the area of hornblendite decomposition, and this resulted in melts that had small melting degrees and were enriched in water-bearing fluids. Due to their insignificant viscosity, these melts could be readily extracted from the mantle source. The high oxygen fugacity in the mantle wedge (as a consequence of the action of fluids from the "oxidized" mantle) was favorable for the saturation of the melts (that had a small melting degrees) in Ti-rich phases (TNT) even at a relatively low Ti concentration. This, in turn, stabilized the HFSE concentrations. Hence, the lavas of the Kirganik Formation in Kamchatka could be produced by the mixing of melts that were characterized by small melting degrees and were enriched in incompatible elements with silica-saturated melts of high melting degrees (derivatives of a MORB source) in a "mantle pudding" environment (Morris and Hart, 1983).

CONCLUSIONS

1. The distribution of incompatible elements and their ratios in rocks of the volcanic series (shoshonitic and potassic alkaline) and the intrusive complex in central Kamchatka (for example, in the differentiated gabbro–syenite and trachybasalt–latite pairs) testify that the rocks of the volcano-plutonic association are comagmatic and the parental melts were derived from a single source.

2. The low HFSE concentrations (compared with those in MORB) and the low Sr and high Nd isotopic ratios suggest that the melts were derived from a source in the depleted mantle.

3. The enrichment of the rocks in LILE indicates that fluid was introduced into the primary magma during its evolution.

ACKNOWLEDGMENTS

This study was supported by the Russian Foundation for Basic Research (project nos. 95-05-14528 and 99-05-65462) and the International Association for the Promotion of Cooperation with Scientists from the

New Independent States of the Former Soviet Union (grant no. 94-31-29).

REFERENCES

Aktivnye vulkany Kamchatki (Active Volcanoes of Kamchatka), Fedotov, S.A. and Masurenkov, Yu.P., Eds., Moscow: Nauka, 1991.

Aslan, Z., Aslan, Z., Sen, C., *et al.*, Rift Related Arc Volcanism during Liassic Time in the Southern Zone of Eastern Pontide Arc, NE Turkey, *J. Abstr. Int. Geochem. Goldschmidt Conf. 2000*, 2000, vol. 5, no. 2, p. 157.

Bloomer, S.H., Stern, R.J., Fisk, E., *et al.*, Shoshonitic Volcanism in the Northern Mariana Arc. 1. Mineralogic and Major and Trace Element Characteristics, *J. Geophys. Res.*, 1989, vol. 94, pp. 4469–4496.

Churikova, T., Dorendorf, F., and Wörner, G., Sources and Fluids in Mantle Wedge below Kamchatka, Evidence from Across-Arc Geochemical Variation, *J. Petrol.*, 2000 (in press).

Davidson, J.P., Isotopic and Trace Element Constraints on the Petrogenesis of Subduction-Related Lavas from Martinique, Lesser Antilles, *J. Geophys. Res.*, 1986, vol. 91, pp. 5943–5962.

Edward, C.M.H., Menzies, M.A., Thirlwall, M.F., *et al.*, The Transition to Potassic Alkaline Volcanism in Island Arcs: The Ringgit–Beser Complex, East Java, Indonesia, *J. Petrol.*, 1994, vol. 35, pp. 1557–1595.

Ellam, R.M., Hawkesworth, C.J., Menzies, M.A., *et al.*, The Volcanism of Southern Italy: Role of Subduction and the Relationship between Potassic and Sodic Alkaline Magmatism, *J. Geophys. Res.*, 1989, vol. 94, pp. 4589–4601.

Fedorov, P.I. and Dubik, F.Yu., The Geochemistry of Late Cretaceous Shoshonite Association of Central Kamchatka, *Izv. Akad. Nauk SSSR, Ser. Geol.*, 1990, no. 3, pp. 30–39.

Fedorov, P.I. and Kazimirov, A.D., The Mineralogy and Geochemistry of Island-Arc Picrites: Evidence from the Southern Part of the Olyutorskii Zone, Koryak Upland, *Dokl. Akad. Nauk SSSR*, 1989, vol. 306, no. 2, pp. 456–460.

Flerov, G.B. and Koloskov, A.V., *Shchelochnoi bazal'tovyi magmatizm Tsentral'noi Kamchatki* (Alkali Basalt Magmatism of Central Kamchatka), Moscow: Nauka, 1976.

Flerov, G.B. and Seliverstov, V.A., Mineralogy and Petrology of Late Cretaceous–Paleogene Potassic Volcanics of Central Kamchatka, *Volkanol. Seismol.*, 1999, no. 6, pp. 3–21.

Flerov, G.B., Koloskov, A.V., and Moskaleva, S.V., Leucite and Analcime in the Late Cretaceous and Paleogene Potassic Basaltoids of Central Kamchatka, *Dokl. Ross. Akad. Nauk*, 1998, vol. 362, no. 1, pp. 87–89.

Geokhimicheskaya tipizatsiya magmaticheskikh i metamorficheskikh porod Kamchatki (Geochemical Typification of Kamchatka Igneous and Metamorphic Rocks), Krivenko, A.P., Ed., Novosibirsk: Inst. Geol. Geofiz. Sib. Otd. Akad. Nauk SSSR, 1990.

Gill, J.B., Geochemistry of Viti Levu, Fiji, and Its Evolution as an Island Arc, *Contrib. Mineral. Petrol.*, 1970, vol. 27, no. 3, pp. 179–203.

Gill, J.B., *Orogenic Andesites and Plate Tectonics*, Berlin: Springer, 1981.

Gill, J.B. and Whelan, P., Early Rifting of an Oceanic Island Arc (Fiji) Produced Shoshonitic to Tholeiitic Basalts, *J. Geophys. Res.*, 1989, vol. 94, no. 4, pp. 4561–4578.

Green, D.H. and Lus, W., Phase Relations and Magmatism in the Mantle Wedge above Subduction Zones, *J. Abstr. Int. Geochem. Goldschmidt Conf. 2000*, 2000, vol. 5. no. 2, p. 454.

Hart, S.R., Heterogeneous Mantle Domains: Signatures, Genesis and Mixing Chronologies, *Earth Planet. Sci. Lett.*, 1988, vol. 90, pp. 273–296.

Houseman, G.A. and Elgland, P., Crustal Thickening Versus Lateral Expulsion in the Indian–Asian Continental Collision, *J. Geophys. Res.*, 1992, vol. 98, pp. 12233–12249.

Irvine, T.N. and Baragar, W.R.A., A Guide to the Chemical Classification of the Common Volcanic Rocks, *Can. J. Earth Sci.*, 1971, vol. 8, pp. 523–548.

Irving, A.J., Petrology and Geochemistry of Composite Ultramafic Xenoliths in Alkalic Basalts and Implications for Magmatic Processes within the Mantle, *Am. J. Sci.*, 1980, vol. 280, pp. 389–426.

Kepezhinskas, P.K., Diverse Shoshonite Magma Series in the Kamchatka Arc: Relationships between Intra-Arc Extension and Composition of Alkaline Magmas, in *Volcanism Associated with Extension at Consuming Plate Margins. Geol. Soc. London Spec. Publ.*, 1995, vol. 81, pp. 249–264.

Kersting, A.B. and Arculus, R.J., Pb Isotope Composition of Klyuchevskoy Volcano, Kamchatka, and North Pacific Sediments: Implications for Magma Genesis and Crustal Recycling in the Kamchatka Arc, *Earth Planet. Sci. Lett.*, 1995, vol. 136, pp. 133–148.

Koloskov, A.V., Problems of Consanguinity of Igneous Rocks from Ophiolitic Associations, in *Vzaimosvyaz' raznoglubinnogo magmatizma* (Correlation of Magmatism from Different Depths), Moscow: Nauka, 1982, pp. 43–61.

Koloskov, A.V., Flerov, G.B., and Golubev, V.N., Sr and Nd Isotope Compositions of Clinopyroxenes from the Late Cretaceous and Paleogene Alkaline Igneous Rocks of Central Kamchatka (Initial Data), *Dokl. Ross. Akad. Nauk*, 2001, vol. 376, no. 1 (in press).

Koloskov, A.V., Flerov, G.B., Seliverstov, V.A., *et al.*, Potassic Volcanics of Central Kamchatka and the Late Cretaceous and Paleogene Kuril–Kamchatka Alkaline Province, *Petrologiya*, 1999, vol. 7, no. 5, pp. 559–576.

Kontak, D.J., Clark, A.H., Farrar, E., *et al.*, Petrogenesis of a Neogene Shoshonite Suite, Cerro Moromoroni, Puno, Southeastern Peru, *Can. Mineral.*, 1986, vol. 24, part 1, pp. 117–135.

Leonova, L.L. and Flerov, G.B., Geochemistry of the Alkaline Rocks of Central Kamchatka, *Geokhimiya*, 1977, no. 1, pp. 82–92.

Lin, P.-N., Stern, R.J., and Bloower, S.H., Shoshonitic Volcanism in the Northern Mariana Arc. 2. Large-Ion Lithophile and Rare Earth Element Abundances: Evidence for the Source in Compatible Element Enrichments in Intraoceanic Arcs, *J. Geophys. Res.*, 1989, vol. 94, no. 4, pp. 4497–4514.

Magmaticheskie gornye porody. T. 6. Evolyutsiya magmatizma v istorii Zemli (Igneous Rocks. Vol. 6: Evolution of Magmatism in the Earth's History), Moscow: Nauka, 1987.

Markovskii, B.A. and Rotman, V.K., On the Geosyncline Meymechite from Kamchatka, *Dokl. Akad. Nauk SSSR*, 1971, vol. 196, no. 3, pp. 675–678.

Meen, J.K., Formation of Shoshonites from Calcalkaline Basalt Magmas: Geochemical and Experimental Constraints

from the Type Locality, *Contrib. Mineral. Petrol.*, 1987, vol. 97, pp. 333–351.

Morris, J.B. and Hart, S.R., Isotopic and Incompatible Element Constraints on the Genesis of Island Arc Volcanics from Cold Bay and Amak Island, Aleutians and Implications for Mantle Structure, *Geochim. Cosmochim. Acta*, 1983, vol. 47, no. 11, pp. 2015–2030.

Nicholls, I.A. and Whitford, D.J., Potassium-rich Volcanic Rocks of the Muriah Complex, Java, Indonesia, Products of Multiple Magma Sources? *J. Volcanol. Geotherm. Res.*, 1983, vol. 18, pp. 337–359.

Pallister, J.S. and Knight, R.J., Rare-Earth Element Geochemistry of Samail Ophiolites near Ibru, Oman, *J. Geophys. Res.*, 1981, vol. 86, pp. 2673–2697.

Peccerillo, A. and Taylor, S.R., Geochemistry of Eocene Calc-Alkaline Volcanic Rocks from the Kastamonu Area, Northern Turkey, *Contrib. Mineral. Petrol.*, 1976, vol. 58, pp. 63–81.

Rogers, N.W., Hawkesworth, D.P., Parker, R.J., *et al.*, The Geochemistry of Potassic Lavas from Vulsini, Central Italy, and Implications for Mantle Enrichment Processes Beneath the Roman Region, *Contrib. Mineral. Petrol.*, 1985, vol. 90, pp. 244–257.

Seliverstov, V.A., Koloskov, A.V., and Chubarov, V.M., Lamproite-like Potassic Ultramafic Alkaline Rocks of the Valaginskii Range, Eastern Kamchatka, *Petrologiya*, 1994, vol. 2, no. 2, pp. 197–213.

Sun, S.-S. and McDonough, W.F., Chemical and Isotopic Systematics of Oceanic Basalts, *Magmatism in Ocean Basin. Geol. Soc. Spec. Publ.*, 1989, vol. 42, pp. 313–345.

Tomson, I.N. and Seliverstov, V.A., Magmatism and Metallogeny of the Preorogenic Tectonic Regime of Mobile Belts and Cratons, *Geol. Rudn. Mestorozhd.*, 1992, vol. 34, no. 3, pp. 3–18.

Tsvetkov, A.A., Volynets, O.N., and Bailey, J., Shoshonites of the Kuril–Kamchatka Island Arc, *Petrologiya*, 1993, vol. 1, no. 2, pp. 123–151.

Turner, S.N., Arnaud, N., Liu, J., *et al.*, Postcollision, Shoshonitic Volcanism on the Tibetan Plateau: Implications for Convective Thinning of the Lithosphere and the Source of Ocean Island Basalts, *J. Petrol.*, 1996, vol. 37, pp. 45–71.

Vinogradov, V.I., Grigor'ev, V.S., and Pokrovskii, B.G., Isotope Composition of Oxygen and Strontium from the Rocks of the Kuril–Kamchatka Island Arc and the Problem of Island Arc Magma Origin, in *Evolyutsiya sistemy kora-mantiya* (Evolution of the Crust–Mantle System), Moscow: Nauka, 1986, pp. 78–102.

Volynets, O.N., Geological Types, Petrology, and Genesis of Late Cenozoic Volcanic Rocks from the Kuril–Kamchatka Island Arc System, *Int. Geol. Rev.*, 1994, vol. 36, no. 4, pp. 373–405.

Volynets, O.N., Anoshin, G.N., and Antipin, V.S., Petrology and Geochemistry of Alkaline and Subalkaline Lavas as an Indicator of Geodynamic Regime in Island Arcs, *Geol. Geofiz.*, 1986, no. 8, pp. 10–17.

Volynets, O.N., Anoshin, G.N., and Puzankov, Yu.M., The Potassic Basaltoids of Western Kamchatka as a Manifestation of Lamproite Group Rocks in an Island Arc System, *Geol. Geofiz.*, 1987, no. 11, pp. 41–51.

Whitford, D.J., White, W.M., and Jezek, P.A., Neodymium Isotopic Composition of Quaternary Island Arc Lavas from Indonesia, *Geochim. Cosmochim. Acta*, 1981, vol. 45, pp. 989–995.